Free-Solution, Label-Free Molecular Interactions Studied by Back-Scattering Interferometry

Darryl J. Bornhop,[1]* Joey C. Latham,[2] Amanda Kussrow,[1] Dmitry A. Markov,[3] Richard D. Jones,[1] Henrik S. Sørensen[4]

Free-solution, label-free molecular interactions were investigated with back-scattering interferometry in a simple optical train composed of a helium-neon laser, a microfluidic channel, and a position sensor. Molecular binding interactions between proteins, ions and protein, and small molecules and protein, were determined with high dynamic range dissociation constants (K_d spanning six decades) and unmatched sensitivity (picomolar K_d's and detection limits of 10,000s of molecules). With this technique, equilibrium dissociation constants were quantified for protein A and immunoglobulin G, interleukin-2 with its monoclonal antibody, and calmodulin with calcium ion Ca^{2+}, a small molecule inhibitor, the protein calcineurin, and the M13 peptide. The high sensitivity of back-scattering interferometry and small volumes of microfluidics allowed the entire calmodulin assay to be performed with 200 picomoles of solute.

Measurement of the rate and affinity of biomolecular interactions, such as protein-protein binding or binding of small molecules, not only provides insight into basic cellular function but also can facilitate the development of therapeutics and serve as the basis for many diagnostic techniques. For measurements at very low concentrations, detection of molecules often requires labeling (such as fluorescent tags), but label-free studies can be performed in two main ways. Calorimetric methods, such as isothermal titration calorimetry (ITC) (*1*–*3*), are performed with all components in solution and have found relatively widespread acceptance. However, these methods have very low throughput, require large sample volumes (milliliters), and have low sensitivity (Table 1) (in the worst case, there is no sensitivity if the reaction enthalpy is near zero). The enthalpic array (*4*) has been used as a high-throughput embodiment of the microcalorimeter and can be used to perform homogeneous, label-free molecular interaction measurements with just 500 nl of sample. Yet the method suffers from poor concentration detection limits (~5×10^{-5} M) (Table 1) restricting the range of measurable binding affinities.

A larger group of related methods relies on immobilizing one of the binding partners to a surface. Several methods, including diffraction, interferometry, wave guiding and plasmon sensing, nanowire sensing (*5*), and microcantilever sensing (*6*), can then be used to detect changes in the surface layer. Although these surface methods are much more sensitive than calorimetry (for typical proteins of interest, detection limits for dissociation constant measurements are 1 to 100 pM versus 1 to 10 nM), surface immobilization of binding partners can raise several issues. The molecule's binding site may be near the surface (*7*) and may induce steric hindrances that could influence the binding energetics and/or kinetics. Surface preparation can be laborious, time-consuming, expensive to implement, and incompatible with some materials, and the surface layers often exhibit decreased activity over time (*8*). Finally, it is not possible to study unknown binding partners or binding partners that are not isolated in quantities sufficient for modification so that they can be bound to surfaces.

We now show that back-scattering interferometry (BSI), which we have previously used with surface immobilization methods (*9*, *10*), can now be used to measure a wide dynamic range (K_d spanning six decades) of molecular interactions in free solution. It provides high sensitivity (picomolar K_d and detection limits of tens of thousands of molecules), either through kinetic or end-point analysis of concentration-dependent binding data. Compatibility with microfluidics gives BSI the added advantage that either assay format can be done on small sample quantities, allowing the study of molecules that require labor-intensive synthesis or are prepared by tedious mutation or isolation methods.

Interferometry is one of the most sensitive optical interrogation methods known and has been used to screen molecular interactions in surface-binding modes. Examples include on-chip embodiments of a Mach-Zehnder (*11*–*14*) and Young Interferometer (*15*), dual polarization interferometer (*16*), porous Si (*17*) and nanoporous Al (*18*) sensors, diffraction optics technology (*19*), and the biological compact disk (BioCD) (*20*, *21*), as well as BSI (*9*, *10*, *22*). The Mach-Zehnder and Young dual polarization interferometers use wave guiding to monitor binding with surface interaction sensing, which requires relatively long sections of the channel to be coated with the target and large sample volumes to be introduced to facilitate micromolar to nanomolar detection limits. The BioCD is based on a disk that has a mirrored surface upon which periodic patterns of proteins can be bound, providing a periodic reflectance pattern that is phase modulated, changing in proportion to the surface bound mass. Porous Si and Al sensors depend on spectral fringe shifts and are limited to monitoring interactions near the surface where the target is attached. We recently demonstrated that BSI, implemented with a fast Fourier transform (FFT) fringe pattern interrogation approach, could be performed in poly(dimethylsiloxane) (PDMS) chips with rectangular channels. This system enabled substrate-immobilized, reversible, label-free molecular interactions on-chip (*9*, *10*). A three base pair mismatch was quantified, and the interaction between protein A and immunoglobulin G (IgG) was monitored at the attomole level (*10*). BSI (Fig. 1) has been effectively performed with cylindrical objects such as fused silica capillaries (*22*), semicircular shaped channels formed from isotropic etching of fused silica (*23*, *24*), and recently with rectangular channels (*9*, *10*). The latter shape was inspired by the simplicity of microfluidic chip production using PDMS (*25*).

Although it is well established that changes in refractive index (RI) at surfaces can be used to study molecular interactions (*9*, *10*, *26*, *27*), some studies (e.g., *28*) suggest that molecular interactions can be quantified in free solution by using an intrinsic signal other than temperature, as in ITC. Sota *et.al.* (*28*) used molar ellipticity of the sample molecule in combination with surface plasmon resonance (SPR), also an RI detector, to show a relation between surface and bulk signals. The underlying implication of their observations may be that an RI detector could be used to measure binding events in free solution. They show that SPR is sensitive to protein conformational changes and waters of hydration, but they also described their results as "counterintuitive." Other studies

Table 1. A comparison of free-solution, label-free molecular interaction techniques.

Technique	Compatibility with μ-fluidics	Minimum sample volume	Detection limits
Microcal ITC (*3*)	No	1.3 mL	1.0×10^{-6} M (1.3 nmol)
Enthalpy arrays (*4*)	No	500 nL	5.0×10^{-5} M (25 pmol)
BSI	Yes	350 pL	8.57×10^{-11} M (30 zmol)

[1]Department of Chemistry, Vanderbilt Institute of Chemical Biology, Vanderbilt University, VU Station B 351822, Nashville, TN 37235–1822, USA. [2]Department of Biochemistry, Vanderbilt University School of Medicine, 465 21st Avenue South, Suite 9160 MRBIII, Nashville, TN 37232, USA. [3]Department of Biomedical Engineering and Vanderbilt Institute for Integrative Biosystems Research and Education (VIIBRE), Vanderbilt University, 5824 Stevenson Center, Nashville, TN 37235, USA. [4]Optics and Plasma Research Department, Risø National Laboratory, Technical University of Denmark, Building 128, Frederiksborgvej 399–DK-4000-Roskilde, Denmark.

*To whom correspondence should be addressed. E-mail: darryl.bornhop@vanderbilt.edu

have shown that it is possible to measure the intrinsic properties of a solute, such as the molecular dipole or polarizability. Elkashef (*29*) used a dual-wavelength interferometer to measure structural properties of laser dye solvents (*29*) and Maroulis *et al*. (*30*) used RI measurements to study dipole, dipole-quadrupole, and dipole-octopole polarizability of adamantane (*30*). Given these findings, we suspected that structural modifications, as in ion-induced protein folding, protein-protein interactions, and small molecule-protein binding events, must be measurable using RI techniques. We now show that BSI can be implemented in free-solution and can detect a 25 pM binding event using a simple optical train based on a PDMS microfluidic chip.

Modeling of the physical mechanism behind the BSI optical phenomenon (*23*, *31*–*33*) indicates that a multipass configuration leads to a long effective path-length and high sensitivity. Impinging coherent parallel rays from a fiber-coupled He-Ne laser beam onto a micrometer-dimensioned rectangular channel in the PDMS chip produces a fan of scattered light. It contains a set of very high contrast interference fringes (Fig. 1A) and results from this beam-channel-fluid interaction. As the composition or RI of the medium contained within the channel changes, these fringes shift spatially (Fig. 1C). The transducer design (*10*) uses a high-resolution linear charge-coupled device and an FFT, which gives a readout in near-real time of the phase for a particular fringe frequency. Spatial phase detection methods allow us to measure RI change to greater than one part per million in picoliter volumes of solution.

The chip contains a serpentine and a squeeze for rapid mixing (Fig. 1B). We adopted a modified "stop-flow" methodology (*34*), configured with two sample reservoirs, both connected to equal-length channels that converge into a single channel with a serpentine mixer made from a series of connected C shapes followed by a restriction (Fig. 1B). This simple microfluidic network, which allows for sample introduction and rapid mixing of the two interacting species, was fabricated using standard photolithography and replica molding techniques (*25*, *35*, *36*). It has a 50 μm by 70 μm rectangular channel that, when interrogated by the 100 μm diameter He-Ne laser beam, yields an optical probe volume of ~350 pL. Stop-flow determinations (*37*) and a simple kinetic model allow us to estimate dissociation constants K_d for an array of binding pairs, which are comparable to end-point determinations. A conservative estimate of the quantifiable signal over background for the antibody-antigen interaction studied here [interleukin-2 (IL-2) with its antibody, and applying a 0.3 s electronic filter for data smoothing] demonstrates that there are just 21 zeptomoles of IL-2 or 12,600 molecules and 0.6 attomoles of the antibody within the probe volume. Our calmodulin (CaM) results show that a species with nanomolar affinity can be assayed with just nanograms (picomoles) to micrograms (nanomoles) of protein or small molecule, which represents the use of one-thousandth the number of species required by ITC.

Because BSI is a highly sensitive RI detector, it is possible that the source of our observed signal was a temperature-induced RI change. However, the signals we measured changed during the course of reaction and then leveled off and remained constant after equilibrium had been reached. Thus, the signals must arise through a permanent change in the RI, because the heat sink would have quickly removed the reaction-generated heat from the chip and fluid and then returned the signal to the original value. A calculation presented in the supporting information (*38*) illustrates that even under the best-case scenario (i.e., the highest concentration of binding pairs), the temperature change resulting from the reaction in aqueous media would not produce a detectable signal in BSI. Even if the reaction produced a temperature change 10 times as high (resulting in a $\Delta RI = 10^{-8}$), our current detection limit of about $\Delta RI = 10^{-6}$ would not facilitate registration of the event.

Having ruled out thermal RI changes as a signal source, we still must account for the source of the binding signal in BSI. We note that binding

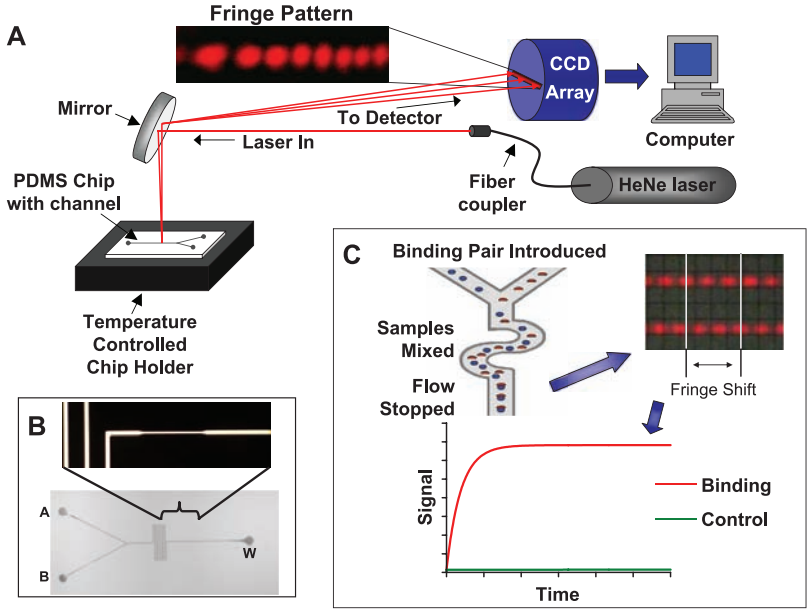

Fig. 1. (**A**) Experimental setup for BSI. (**B**) Microfluidic chip with serpentine mixer and restriction. (**C**) Photograph of representative fringe patterns showing a RI-induced position shift of the fringes, a representation of a binding event, and observed signal for a control and reactive pair binding event.

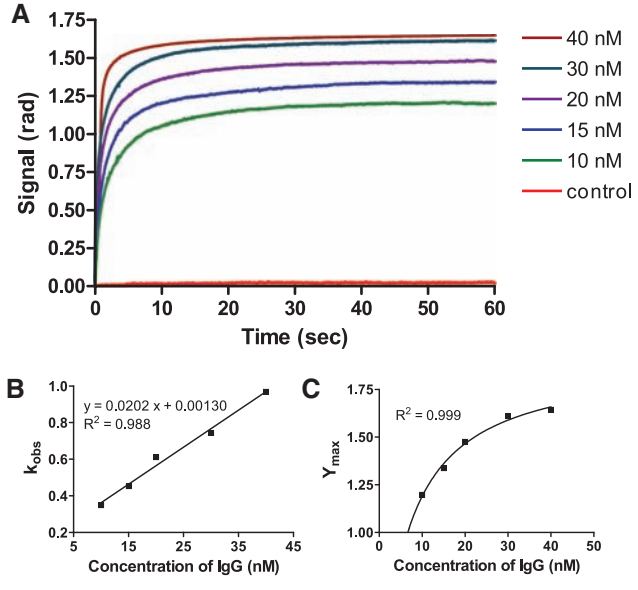

Fig. 2. (**A**) Real-time association plots are shown for P_A binding IgG at various nanomolar concentrations. In the stop-flow interaction experiments, a fixed concentration of 2.5 nM P_A was used, and sequential experiments with increasingly larger concentrations of the F_C region from IgG (i.e., from 10 to 40 nM) were performed. P_A was buffered at a pH = 7.2 with 15 mM Na_2HPO_4, 50 mM NaCl, 0.1 mM EGTA, and 0.02% sodium azide. All IgG solutions were made using the same buffer as P_A. The temperature of the solutions and microfluidic chip were held constant at 25°C ± 0.01°C throughout the experiment. (**B**) Extracted rates are plotted versus IgG concentration. (**C**) End-point values are plotted as a function of IgG concentration and analyzed by Prism software.

creates a new entity in solution that may have a very different refractive index (RI) or molecular dipole from that of either of the reacting analytes. We are not measuring the combined RI or sample mixing (fig. S7) (*38*) because there is virtually no measurable "binding event" signal produced by the controls. The effect of waters of hydration on the intrinsic dipole of a forming complex or folding protein are underestimated and could be a major contributing factor in BSI. For example, during Ca^{2+}-induced folding of CaM, many water molecules (>35/CaM molecule) are ejected from the compound (*39*). Such an event most certainly produces substantial electrostatic effects leading to a highly modified molecular dipole relative to that of the unfolded compound.

We now describe our results for several typical binding experiments. Protein A (P_A) binds the F_C region of several IgG species, including human and rabbit, with high affinity (K_d values from 5 to 34.5 nM) (*40*, *41*). The association reaction was monitored in real time during an interval of ~60 s. As expected, the "shape" of the binding curves changed and more rapidly reached the equilibrium point at higher concentrations of the antibody (IgG) at fixed concentration of the substrate (receptor).

The apparent binding affinity can be extracted from the data using a simple model that assumes first-order kinetics or single-mode binding (*38*) and plotting the observed rate (k_{obs}) versus the concentration of IgG (Fig. 2B). Least-squares analysis of the line generated by this method from the kinetics obtained from BSI yields a K_d for P_A-IgG of 7.92 nM (±1.71). Alternatively, a plot of the end-point values of phase for the reaction between P_A and IgG as a function of the concentration of IgG can be used as a second method to evaluate binding affinity of the complex. This plot (Fig. 2C) exhibits the expected hyperbolic shape often seen in enzyme kinetic studies and described by the law of mass action. Analysis of the end point yields a K_d value of 6.05 nM (±0.52), which correlates well with the results obtained from the kinetic analysis and with reported values (*41*). The quasi leveling-off observed at higher concentrations of the ligand in the end-point assay is attributed to a bulk RI signal, which becomes increasingly significant at higher concentrations of the ligand, IgG. Although this background signal is always present in the BSI experiment, we have studied its magnitude and have determined that the contribution is small compared with that of the binding event (3 to 5%, depending on the concentration and RI of the reacting species).

The control shown in Fig. 2A illustrates the result for mixing the 2.5-nM solution of P_A with a 40-nM solution of the F_{AB} fragment of IgG (rather than the F_C region) and shows that combining a high concentration of the noncomplementary receptor with the target results in a nominal response by BSI. The control shows <1.6% of the signal observed at equivalent P_A and IgG F_C concentrations and exhibits decidedly different kinetics. Although a bulk property change is expected and observed, the magnitude of this contribution is small.

The interaction assays by BSI benefit from the inherent advantages afforded by microfluidics, as

Table 2. The binding affinities determined by BSI compared with reported values.

Binding partners	K_d BSI		Reported	Detection method of published data
	Kinetic	Endpoint		
CaM-Ca^{2+}	3.40 μM	18.23 μM	1–10 μM	Equilibrium and flow dialysis (*43*)
CaM-TFP	4.73 μM	7.82 μM	4.5–5.8 μM	Affinity chromatography (*44*)
CaM-CaN	15.64 nM	11.39 nM	4–16 nM	Radioisotope (*46*, *47*) and affinity chromatography (*45*)
CaM-M13	2.89 nM	9.87 nM	1.9–5.5 nM	SPR (*48*)
P_A-IgG	7.92 nM	6.05 nM	5–34.5 nM	Acoustic waveguide (*41*) and others (*40*)
IL-2-Ab	25.91 pM		10–60 pM	Radioisotope (*52*)

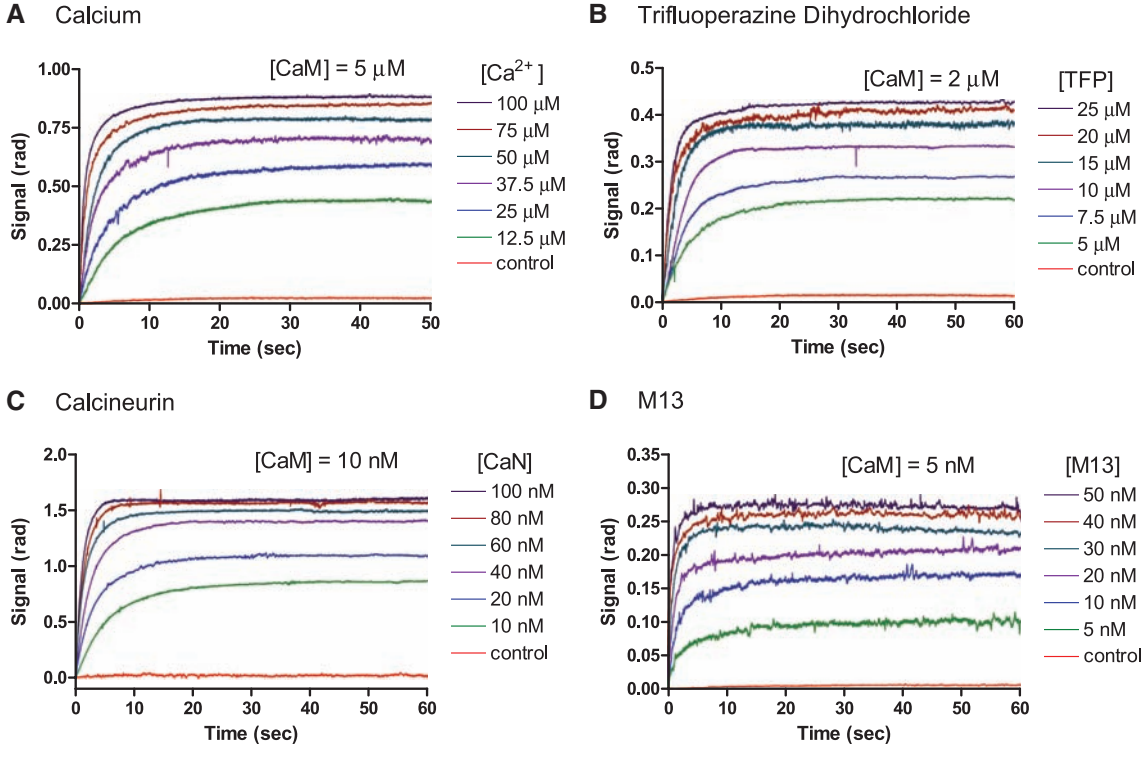

Fig. 3. Association curves of CaM with (**A**) Ca^{2+} using a constant buffered concentration of 5 μM CaM and Ca^{2+} concentrations from 12.5 to 100 μM. All CaM solutions used contained a small amount of EGTA to chelate any free Ca^{2+}. A 5 μM CaM solution and a 100 μM Ca^{2+} solution, both containing excess EGTA (i.e., 400 μM), served as the control. (**B**) TFP using a constant concentration of 2 μM activated CaM. TFP solutions were made in the same buffer and held at the same pH as CaM. A 2 μM solution of CaM and a 25 μM solution of TFP, both in the absence of Ca^{2+}, were mixed to serve as a control. (**C**) Calcineurin using a constant concentration of 10 nM activated CaM and a control of 10 nM solution of CaM and a 100 nM solution of Calcineurin, both in the absence of Ca^{2+}. (**D**) M13 using a concentration of activated CaM kept constant at 5 nM. A 5 nM solution of CaM and a 50 nM solution of M13, both devoid of CaM activating Ca^{2+} served as the control.

was also the case for entire syntheses performed on-chip (*42*). The macro-micro interface is less than optimal for our system, yet it was possible to perform the entire P_A-IgG binding assays with only 105×10^{-9} g (2.5 pmol) of P_A and just 287×10^{-9} g (5.75 pmol) of the F_C fragment of IgG. Under the best-case scenario, a comparable determination by ITC would require 300 to 1000 times as much mass (~ 300 μg) of each of the reactants.

We chose CaM, the ubiquitous calcium-binding protein that can bind to and regulate a multitude of different protein targets, to further demonstrate the utility of BSI. Upon binding to Ca^{2+}, CaM undergoes a conformational change thought to induce activity. Once activated by Ca^{2+}, CaM binds, among other targets, the protein calcineurin, a skeletal muscle myosin peptide, and small inhibitor molecules. Ligands ranging in size from ions such as Ca^{2+} to 77 kD proteins and spanning three decades in K_d (from a few micomolar to tens of nanomolar) provide an array of ligand-substrate interactions to evaluate BSI methodology. We quantified (i) CaM-Ca^{2+} interactions, (ii) interactions between CaM and the small-molecule inhibitor trifluoperazine dihydrochloride (TFP), (iii) CaM-calcineurin binding, and (iv) reactions of CaM with M13, a peptide from the sequence of skeletal muscle myosin light chain kinase (sk-MLCK), a known target of the Ca^{2+}-activated CaM complex. In all of these experiments performed at 25°C, the CaM solutions were buffered. For the latter three studies, CaM was activated with Ca^{2+}, and unactivated CaM, in the absence of Ca^{2+}, served as a control. The values reported previously and those we have measured are summarized in Table 2.

The reported K_d values for CaM-Ca^{2+} range from 1 to 10 μM (*43*). The control showed < 3% change in signal above that observed in the absence of excess EGTA at equivalent CaM and Ca^{2+} concentrations (Fig. 3A). Kinetic analysis with a single exponential gives rise to a plot of observed rates versus Ca^{2+} concentration that is linear (*38*). A linear least-squares analysis of the data gives the slope, the intercept, and their respective uncertainties. From this analysis, K_d was determined to be 3.40 μM (±2.86). Analysis of the plot of the end-point values monitored by BSI versus the concentration of Ca^{2+} yields a K_d value of 18.23 μM (±1.43), which is above the range previously reported. The disparity in these two values may arise from the use of an overly simplistic model of the reaction kinetics (for example, Ca^{2+} is known to bind more than one CaM site) and/or from the RI background present from unreacted ligand, particularly at high concentrations. Even four-site binding models provide questionable fits of kinetic data for this system (*43*).

The interaction between CaM and TFP was previously examined with affinity chromatography (*44*). This method required 30 μg per sample, with each sample analysis requiring 300 μl. In these chromatography studies, dissociation constants or affinities ranged from 4.5 to 5.8 μM. At equivalent CaM and TFP concentrations, the control showed <4% of the signal observed when Ca^{2+} was present (Fig. 3B). Kinetic analysis produces a linear relation between the observed rates over the concentration range of TFP used (*38*), and from the least-squares analysis, K_d was determined to be 4.73 μM (±0.48) for the CaM-TFP complex, which is within the range obtained by affinity chromatography (*44*). A plot of the BSI signal values at end-point versus TFP concentration was constructed and gave a K_d of 7.82 μM (±0.91).

Calcineurin is a protein phosphatase and the major CaM binding protein in the brain (*45*). The pair has been studied previously using both affinity chromatography and radioligand binding (*45*–*47*), with reported K_d's between 4 and 16 nM. The unactivated control showed <1.5% of the signal observed at the equivalent CaM and calcineurin concentrations in the presence of Ca^{2+} (Fig. 3C). Kinetic analysis yields a linear relation between the observed rates and calcineurin concentration (*38*). The slope and intercept from a least-squares analysis yields a K_d of 15.64 nM (±3.24), again within the range of reported values from affinity chromatography and radioligand binding (*45*–*47*). End-point analysis yielded a hyperbolic relation (*38*) and a K_d of 11.39 nM (±0.82).

M13, a peptide from sk-MLCK, is also a known target of the Ca^{2+}-activated CaM complex and has been shown by SPR to bind with high affinity (K_d = 1.9 to 5.5 nM) (*48*). A range of concentrations of M13 were reacted with CaM sequentially, and time-dependent association events were detected by interferometry (Fig. 3D). A control showed <2.6% of the signal observed when Ca^{2+} was present. A linear relation between the observed rates and the ligand concentration (M13) enabled the calculation of K_d. For the CaM-M13 pair, this value was 2.89 nM (±0.74), which compares well with the SPR values (*48*). Analysis with the end-point CaM-M13 signal values versus concentration yields a K_d value of 9.87 nM (±1.12) (*38*). The likely causes for the disparity between the end-point and kinetic affinity values are that this interaction produces less signal, requiring the assay to be done near the noise floor, and a relatively larger noninteraction RI change at higher concentrations of ligand.

Kinetic parameters can also be derived from BSI. For example, the interaction of CaM with M13 showed high consistency with stopped-flow kinetics performed previously (*49*). The association rate determined by BSI was 3.1×10^7 $M^{-1}s^{-1}$, compared with 3.9×10^7 $M^{-1}s^{-1}$ as determined by Török (*49*). Homogeneous assays based on calorimetry are problematic for very low and very high binding affinities. To effectively evaluate the interaction between pairs with picomolar binding affinities, it is desirable to perform the determination at subnanomolar concentrations, which is often not possible with ITC but is well within the range possible with BSI. To demonstrate this capability, we measured the interaction between IL-2 and a monoclonal antibody in buffer (*38*) and in cell-free media (Fig. 4). Activated T cells secrete IL-2 (*50*, *51*), which, among its other roles, is responsible for the proliferation of antigen-specific cells, as well as promoting the proliferation and differentiation of other immune cells. IL-2 and its antibody (IL-Ab) have been shown to bind with high affinity, with reported K_d values ranging from 10 to 60 pM (*52*). BSI was used to monitor real-time interactions IL-Ab with IL-2 in free solution and in cell media. The slight, nearly identical RI change observed for the blank and two controls was attributed to the mixing of the media. The kinetic analysis, as described above for the CaM and P_A- IgG pairs, yields a linear plot (*38*). From the analysis, a K_d of 25.91 pM (±5.24 pM) was determined, which falls within the published range of 10 to 60 pM (*52*).

Although additional work is required to completely understand the intricacies of free-solution interaction determinations by BSI, the observations presented here demonstrate that such measurements can be performed label-free with high sensitivity over a six-decade dynamic range for K_d determinations with values as low as 4 μM and as high as tens of pM. For example, using an unoptimized microfluidic network, the entire CaM study required the consumption of only about 200 picomoles or 3 μg CaM. To perform a similar analysis with ITC would have required about 250 times as much solute, or about 0.8 mg. The lower concentrations used in BSI may avoid errors resulting from solute aggregation. We note that all of the data presented were obtained using a single-channel system and, excluding the IL-2 results, with no active or passive signal filtering. It should also be possible to use this method to look for the presence of unknown binding partners, such

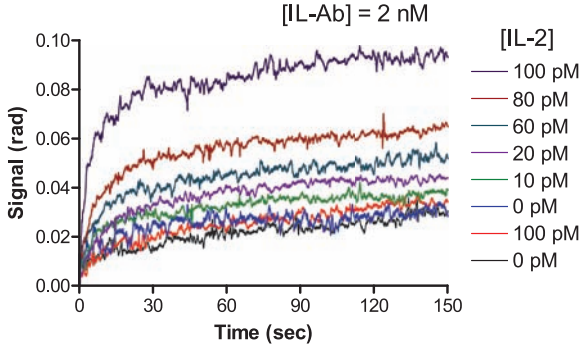

Fig. 4. IL-2-Ab binding curves with interaction assay performed in cell-free media. The IL-Ab concentration was held constant at 2 nM. Both the IL-2 and IL-Ab solutions were made using RPMI 1640 cell media with 1% fetal bovine serum and 10 μg/mL Cipro. A blank [0 M of both IL-2 and IL-Ab, (black)], as well as two controls [0 pM IL-2 reacted with 2 nM IL-Ab (blue); 100 pM IL-2 mixed on chip with 0 nM IL-Ab (red)] were evaluated.

as from cellular extracts, to a target of known concentration.

References and Notes

1. A. Velazquez-Campoy, E. Freire, *Biophys. Chem.* **115**, 115 (2005).
2. A. Ababou, J. E. Ladbury, *J. Mol. Recognit.* **20**, 4 (2007).
3. S. Leavitt, E. Freire, *Curr. Opin. Struct. Biol.* **11**, 560 (2001).
4. F. E. Torres *et al*., *Proc. Natl. Acad. Sci. U.S.A.* **101**, 9517 (2004).
5. J. Hahm, C. M. Lieber, *Nano Lett.* **4**, 51 (2004).
6. G. Shekhawat, S. H. Tark, V. P. Dravid, *Science* **311**, 1592 (2006).
7. M. B. Kerby, R. S. Legge, A. Tripathi, *Anal. Chem.* **78**, 8273 (2006).
8. R. L. Rich, Y. S. N. Day, T. A. Morton, D. G. Myszka, *Anal. Biochem.* **296**, 197 (2001).
9. D. A. Markov, K. Swinney, D. J. Bornhop, *J. Am. Chem. Soc.* **126**, 16659 (2004).
10. J. C. Latham, D. A. Markov, H. S. Sorensen, D. J. Bornhop, *Angew. Chem. Int. Ed.* **45**, 955 (2006).
11. F. Brosinger *et al*., *Sens. Actuators B Chem.* **44**, 350 (1997).
12. F. Prieto *et al*., *Nanotechnology* **14**, 907 (2003).
13. F. Prieto *et al*., *Sens. Actuators B Chem.* **92**, 151 (2003).
14. E. F. Schipper *et al*., *Sens. Actuators B Chem.* **40**, 147 (1997).
15. A. Ymeti *et al*., *Appl. Opt.* **42**, 5649 (2003).
16. M. J. Swann, L. L. Peel, S. Carrington, N. J. Freeman, *Anal. Biochem.* **329**, 190 (2004).
17. Y. Y. Li *et al*., *Science* **299**, 2045 (2003).
18. S. L. Pan, L. J. Rothberg, *Nano Lett.* **3**, 811 (2003).
19. J. B. Goh, R. W. Loo, M. C. Goh, *Sens. Actuators B Chem.* **106**, 243 (2005).
20. M. Zhao *et al*., *Clin. Chem.* **52**, 2135 (2006).
21. J. J. La Clair, M. D. Burkart, *Org. Biomol. Chem.* **1**, 3244 (2003).
22. H. S. Sorensen, N. B. Larsen, J. C. Latham, D. J. Bornhop, P. E. Andersen, *Appl. Phys. Lett.* **89**, 151108 (2006).
23. K. Swinney, D. Markov, D. J. Bornhop, *Anal. Chem.* **72**, 2690 (2000).
24. D. A. Markov, S. Dotson, S. Wood, D. J. Bornhop, *Electrophoresis* **25**, 3805 (2004).
25. D. C. Duffy, J. C. McDonald, O. J. A. Schueller, G. M. Whitesides, *Anal. Chem.* **70**, 4974 (1998).
26. G. J. Wegner, N. J. Lee, G. Marriott, R. M. Corn, *Anal. Chem.* **75**, 4740 (2003).
27. T. Sakai *et al*., *Anal. Sci.* **20**, 279 (2004).
28. H. Sota, Y. Hasegawa, M. Iwakura, *Anal. Chem.* **70**, 2019 (1998).
29. H. Elkashef, *Opt. Mater.* **8**, 175 (1997).
30. G. Maroulis, D. Xenides, U. Hohm, A. Loose, *J. Chem. Phys.* **115**, 7957 (2001).
31. K. Swinney, D. Markov, D. J. Bornhop, *Rev. Sci. Instrum.* **71**, 2684 (2000).
32. H. J. Tarigan, P. Neill, C. K. Kenmore, D. J. Bornhop, *Anal. Chem.* **68**, 1762 (1996).
33. H. S. Sorensen, Thesis, Technical University of Denmark (2006).
34. B. J. Burke, F. E. Regnier, *Anal. Chem.* **75**, 1786 (2003).
35. G. M. Whitesides, E. Ostuni, S. Takayama, X. Y. Jiang, D. E. Ingber, *Annu. Rev. Biomed. Eng.* **3**, 335 (2001).
36. After the PDMS was cured and peeled from the mold, it was oxidized in O_2 plasma for 30 s and then placed on a 1-mm-thick microscope glass slide, creating an irreversible bond between the glass and PDMS. The glass slide was used to seal the microfluidic channels and allowed for the entire chip assembly to be handled and securely mounted onto a thermoelectrically temperature-controlled x-y translation stage. A shorter top piece of glass was also used as a faceplate, offering structural stability to minimize channel deformations during the sample introduction step. Nanoliter volumes of samples of each of the two binding pairs were placed in the reservoirs at the top of the "Y," then a slight negative pressure was applied to the chip exit well, drawing the two interacting species through the mixer and into the detection zone.
37. In our stop-flow experiments, the sample introduction pressure was chosen to optimize the flow rate and mixing of the solutes. The constraints of the mixer system made it necessary to balance the need for rapid, complete mixing to produce a homogeneous solution of the binding pair with the requirement that the reaction has not proceeded appreciably before flow is stopped and analysis begins. These parameters change slightly for each binding pair, with flow rates found to be in the range of 75 to 120 μL/min.
38. Materials and methods are available as supporting material on *Science* online.
39. E. Project, R. Friedman, E. Nachliel, M. Gutman, *Biophys. J.* **90**, 3842 (2006).
40. J. J. Langone, *Adv. Immunol.* **32**, 157 (1982).
41. K. Saha, F. Bender, E. Gizeli, *Anal. Chem.* **75**, 835 (2003).
42. C. C. Lee *et al*., *Science* **310**, 1793 (2005).
43. H. Tsuruta, T. Sano, *Biophys. Chem.* **35**, 75 (1990).
44. L. Massom, H. Lee, H. W. Jarrett, *Biochemistry* **29**, 671 (1990).
45. C. B. Klee, M. H. Krinks, *Biochemistry* **17**, 120 (1978).
46. M. G. Speaker, S. J. Orlow, T. W. Sturgill, O. M. Rosen, *Proc. Natl. Acad.Sci. U.S.A.* **80**, 329 (1983).
47. M. J. Hubbard, C. B. Klee, *J. Biol. Chem.* **262**, 15062 (1987).
48. S. Montigiani, G. Neri, P. Neri, D. Neri, *J. Mol. Biol.* **258**, 6 (1996).
49. K. Török, *Biochem. Soc. Trans.* **30**, 55 (2002).
50. J. Theze, P. M. Alzari, J. Bertoglio, *Immunol. Today* **17**, 481 (1996).
51. A. K. Abbas, A. H. Lichtman, *Cellular and Molecular Immunology* (Saunders, Philadelphia, ed. 5, 2003).
52. G. H. Reem, N. H. Yeh, D. L. Urdal, P. L. Kilian, J. J. Farrar, *Proc. Natl. Acad. Sci. U.S.A.* **82**, 8663 (1985).

53. This research was supported by National Institute of Biomedical Imaging and Bioengineering at NIH, R-01 EB0003537-01A2, Vanderbilt Institute for Chemical Biology, Air Force Office of Scientific Research grants FA9550-04-1-0364 and FA9550-05-1-0349, and the Vanderbilt Institute for Integrative Biosystems and Education, as well as by vision sciences training grant T32-EY07135 and BIOP Graduate School grant 643-01-0092. We thank J. B. Haas for editorial assistance and P. E. Andersen, S. Dotson, S. Faley, R. Flowers, H. Mchaourab, and J. Wikswo for helpful discussions.

Supporting Online Material

www.sciencemag.org/cgi/content/full/317/5845/1732/DC1
Materials and Methods
SOM Text
Figs. S1 to S7
References
Movie S1

15 June 2007; accepted 8 August 2007
10.1126/science.1146559

Asymmetric Catalysis of the Transannular Diels-Alder Reaction

Emily P. Balskus and Eric N. Jacobsen*

Transannular chemical reactions are unparalleled in their ability to generate high degrees of stereochemical and architectural complexity in a single transformation. However, the successful application of this approach in synthesis depends on the ability to predict and control the outcome of the transannular reaction. Use of a chiral catalyst in this context represents an attractive, yet unused, strategy. This report describes a catalytic, asymmetric transannnular Diels-Alder (TADA) reaction that affords polycyclic products in high enantiomeric excess. This catalyst system can also alter the inherent diastereoselectivity of cyclizations with substrates containing chiral centers. Additionally, the catalytic enantioselective TADA has been used as the key step in a total synthesis of the sesquiterpene 11,12-diacetoxydrimane; this route may provide a general approach to the polycyclic carbon framework shared by many terpene natural products.

The challenge of constructing complex molecules has captured the attention of synthetic chemists for over a century. Polycyclic, stereochemically complex carbon frameworks are a common feature of many biologically active synthetic and naturally occurring targets. Among the possible strategies for assembling such compounds, transannular reactions constitute a particularly efficient approach (Fig. 1A). In this type of transformation, reacting centers are tethered together as part of a macrocycle; covalent bond formation occurs across the ring, resulting in the formation of a polycyclic product, often with concomitant formation of multiple stereogenic centers. The relative proximity of the reacting sites can confer an entropic advantage to transannular reactions, allowing reactions within sterically congested frameworks that are effectively inert in analogous inter- or acyclic intramolecular systems. However, successful application of transannular strategies in target-oriented synthesis depends on the ability to predict and influence the stereochemical course of the reaction.

In the vast majority of transannular transformations studied to date, stereoselectivity has relied on the intrinsic conformational properties of the reacting macrocycle. An appealing alternative strategy for controlling enantio- and diastereoselectivity in transannular reactions might involve use of a chiral catalyst or reagent. Despite numerous efforts in this direction, efficient asymmetric catalysis of transannular reactions has not been achieved (*1*–*5*).

The Diels-Alder reaction has long stood as one of the most useful complexity-generating

Department of Chemistry and Chemical Biology, Harvard University, Cambridge, MA 02138, USA.

*To whom correspondence should be addressed. E-mail: jacobsen@chemistry.harvard.edu

Free-Solution, Label-Free Molecular Interactions Studied by Back-Scattering Interferometry

Darryl J. Bornhop, Joey C. Latham, Amanda Kussrow, Dmitry A. Markov, Richard D. Jones and Henrik S. Sørensen

Science **317** (5845), 1732-1736.
DOI: 10.1126/science.1146559